

Marked load-bearing ability of *Mytilus* smooth muscle in both active and catch states as revealed by quick increases in load

Masao Mukou¹, Hirohiko Kishi¹, Ibuki Shirakawa¹, Takakazu Kobayashi², Katsutoshi Tominaga², Haruka Imanishi² and Haruo Sugi^{1,*}

¹Department of Physiology, School of Medicine, Teikyo University, Itabashi-ku, Tokyo 173-8605, Japan and

²Department of Electronic Engineering, Shibaura Institute of Technology, Minato-ku, Tokyo 108-8548, Japan

*Author for correspondence (e-mail: sugi@med.teikyo-u.ac.jp)

Accepted 12 February 2004

Summary

The anterior byssal retractor muscle (ABRM) of the bivalve *Mytilus edulis* shows a prolonged tonic contraction, called the catch state. To investigate the catch mechanism, details of which still remain obscure, we studied the mechanical responses of ABRM fibres to quick increases in load applied during maximum active isometric force (P_0) generation and during the catch state. The mechanical response consisted of three components: (1) initial extension of the series elastic component (SEC), (2) early isotonic fibre lengthening with decreasing velocity, and (3) late steady isotonic fibre lengthening. The ABRM fibres could bear extremely large loads up to 10–15 P_0 for more than 30–60 s, while being lengthened extremely slowly. If, on the other hand, quick increases in load were

applied during the early isometric force development, the ABRM fibres were lengthened rapidly ('give') under loads of 1.5–2 P_0 . These findings might possibly be explained by two independent systems acting in parallel with each other; one is the actomyosin system producing active shortening and active force generation, while the other is the load-bearing system responsible for the extremely marked load-bearing ability as well as the maintenance of the catch state.

Key words: *Mytilus edulis*, smooth muscle, catch state, load-bearing ability, series elastic component, isotonic lengthening, parallel hypothesis.

Introduction

The anterior byssal retractor muscle (ABRM) of a bivalve mollusc *Mytilus edulis* contracts actively in response to acetylcholine (ACh), and on removal of ACh after the maximum isometric force has been reached, goes into a prolonged tonic contraction that is maintained with very little energy expenditure (Nauss and Davies, 1966; Baguet and Gillis, 1968). The prolonged contraction is called the catch state, in which the ABRM fibres neither shorten actively nor redevelop force after a quick release (Jewell, 1959). The catch state is accompanied by a decrease in the intracellular free Ca^{2+} concentration below the level required for activation of the contractile system (Baguet, 1973; Atsumi and Sugi, 1976; Ishii et al., 1989). The ABRM fibres in the catch state can be made to relax using 5-hydroxytryptamine (5-HT) (Twarog, 1954).

There are two different hypotheses to account for the catch mechanism. One is the linkage hypothesis, in which the catch state is associated with a marked decrease in dissociation rate of actin–myosin linkages between the thick and thin filaments (Lowy and Millman, 1963). The other is the parallel hypothesis, which assumes, in addition to the actin–myosin linkages responsible for active force development, formation of linkages interconnecting the paramyosin-containing thick

filaments (Johnson et al., 1959; Heumann and Zebe, 1968). The parallel hypothesis is based on electron microscopic evidence that a marked aggregation of the thick filaments takes place during the catch state (Heumann and Zebe, 1968; Gilloteaux and Baguet, 1977; Hauk and Achazi, 1987). It has been pointed out, however, that the thick filament aggregation may be an artifact resulting from glutaraldehyde fixation (Miller, 1968). In fact, Bennett and Elliott (1989), who used techniques of quick-freezing and freeze-substitution, observed no thick filament aggregation in the ABRM fibres during the catch state. By contrast, using the same techniques of quick-freezing and freeze-substitution, Takahashi et al. (2003) found that linkages interconnecting the thick filaments are associated with the catch state. Thus, the mechanism underlying the catch state still remains obscure.

Since the physiological function of the catch state is to resist externally applied forces, its physiological characteristics may best be understood by studying the load-bearing ability of the ABRM. The present experiments were undertaken to examine mechanical responses of the ABRM fibres to quick increases in load applied at various states. It will be shown that the load-bearing ability of the ABRM fibres is several times larger than

that of skeletal muscle fibres, indicating the presence of the load-bearing system other than the actomyosin system.

Materials and methods

Preparation

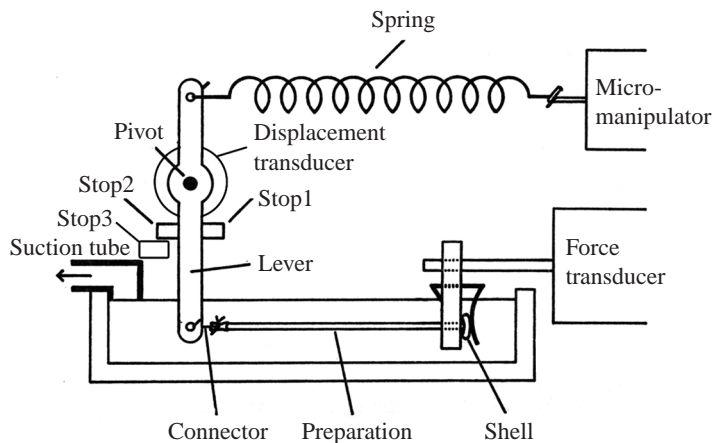
Specimen of *Mytilus edulis* L. were collected at the Misaki Marine Biological Station, Japan, and kept in artificial seawater. The ABRM was isolated with a piece of shell attached to one end and the byssal organ left at the other, and carefully teased to obtain a fibre bundle of 0.5–1 mm diameter. The ABRM fibres were completely relaxed in the presence of 10^{-6} mol l⁻¹ 5-HT. They were placed in an experimental chamber filled with artificial seawater (ASW) containing 513 mmol l⁻¹ NaCl, 10 mmol l⁻¹ KCl, 10 mmol l⁻¹ CaCl₂ and 50 mmol l⁻¹ MgCl₂ (pH adjusted to 7.2 by NaHCO₃ or 10 mmol l⁻¹ Tris maleate), and mounted horizontally between the displacement and the force transducers at ~0.9 times the slack length L_0 (1.8–2.3 cm), i.e. the length at which the resting force was just barely perceptible, to avoid development of resting force during lengthening of the preparation. The large variation in L_0 is due to the variation in animal size. The byssal end of the fibres was hooked to the arm of the displacement transducer, while the shell end was connected to the extension of the force transducer (Fig. 1). Solutions in the chamber were exchanged *via* a water vacuum suction tube.

Transducers

The displacement transducer was a differential transformer (ME Commercial Co., Tokyo, Japan; modulation frequency, 5.5 kHz) with an aluminium lever pivoted on bearings. The distal part of the lever dipped into the experimental solution, and the preparation was connected at a point 3 cm distant from the pivot. The compliance of the lever at the point of attachment of the preparation was $0.5 \mu\text{m g}^{-1}$. The force transducer was a strain gauge (U-gauge, Shinko, Tokyo, Japan) with the compliance of $1 \mu\text{m g}^{-1}$ and the natural frequency of oscillation of ~150 Hz.

General procedure

The experimental arrangement is illustrated in Fig. 1. The



lever of the displacement transducer was initially fixed in position by stops 1 and 2. The preparation was made to contract actively with a supramaximal concentration of acetylcholine (ACh, 10^{-3} mol l⁻¹), and at various times after the onset of force development, the load on the preparation was quickly increased by withdrawing stop 2 electromagnetically, so that the preparation was lengthened under a load imposed by the loading spring. The lengthening of the preparation under a large load was limited to ~10% of L_0 by another stop 3, to avoid damage to the preparation due to a large lengthening, and also to avoid the resting force development during lengthening. The maximum isometric force P_0 ranged from 6 to 25 g.

The preparation was first subjected to a quick increase in load during generation of the maximum ACh-induced isometric force P_0 . After recording the resulting fibre lengthening, the preparation was restored to its original length and ACh was removed to put the preparation into the catch state, which was established 3–5 min after the ACh removal (Sugi et al., 1999). The preparation was then subjected to quick increases in load at various force levels P_x . The experiments were also performed, in which quick increases in load were applied to the preparation in the catch state without preceding quick increases in load at P_0 , with similar results. In some experiments, quick increases in load were applied during the early phase of ACh-induced isometric force development. In some experiments, the length and force changes of the preparation were recorded using an oscilloscope. The length and force changes were complete in 5 ms.

The length and force changes were recorded on an ink-writing oscillograph. After each experiment, the preparation was relaxed by 5-HT (10^{-6} mol l⁻¹), and kept for 5–10 min before it was again stimulated by ACh. All experiments were done at 18–23°C

High-speed cinematography of the segmental length changes of the preparation

To examine whether the mechanical response of the preparation is associated with uniform length changes along the entire length of the preparation, a number of carbon particles were firmly attached to the preparation and the lengths of 5–6 segments between the particles were measured on videotapes taken at 240 frames s⁻¹ with a high-speed video system (FASTCAMrabbit 1, Photron, Tokyo, Japan; Kobayashi et al., 1998) during the experiments.

Fig. 1. Diagram of experimental arrangement. The byssal end of the preparation was hooked to the lower lever of the displacement transducer with a stainless steel wire connector, while the shell end was held with the extension of the force transducer. The lever was initially fixed in position by stops 1 and 2, and after the full development of ACh-induced isometric force, stop 2 was removed to load the preparation with the spring, hooked between the upper lever and the micromanipulator.

Results

Characteristics of mechanical response of the ABRM fibres to quick increases in load

Fig. 2 shows typical records of length (upper traces) and force (lower traces) changes of the ABRM fibres following quick increases in load, applied at the peak of ACh-induced active isometric force P_0 (Fig. 2A) and at the force level P_x during the catch state (Fig. 2B). In both cases, the mechanical responses to quick increases in load from P_0 or P_x to P consisted of the following three phases, as illustrated in the inset; (1) the initial elastic extension of the preparation coincident with the applied force change, (2) the early isotonic lengthening with decreasing velocity, and (3) the late steady isotonic lengthening in which the preparation was lengthened slowly.

The initial elastic extension of the preparation (ΔSEC) is thought to be due to extension of the series elastic component (Tameyasu and Sugi, 1976; Sugi and Tsuchiya, 1979), while the subsequent two phases of isotonic lengthening reflect characteristics of load-bearing structures in the ABRM fibres. We measured the amplitude of the early isotonic lengthening ΔL by extrapolating the late steady lengthening back to the moment of quick load changes (Fig. 2, inset). As the catch force falls gradually with time, the force level P_x at which a quick increase in load was applied during the catch state, ranged from 0.2 to $0.6P_0$.

Marked load-bearing ability of the ABRM fibres in both the active and the catch state

The load-bearing ability of the ABRM fibres was found to be extremely large, both during generation of the maximum ACh-induced active force and during the catch state. As shown in Fig. 3A, the preparation generating the maximum active force P_0 could bear a load up to $10\text{--}15P_0$ for more than 30–60 s without being lengthened rapidly. The marked load-bearing ability contrasts with that of tetanized vertebrate skeletal muscle fibres, which are unable to bear a load above $1.8\text{--}2P_0$ and are lengthened rapidly ('give'; Katz, 1939; Sugi and Tsuchiya, 1981). The marked load-bearing ability of the ABRM fibres was well maintained during the catch state

though the catch forces P_x were much smaller than P_0 . The preparation could bear a load up to $15\text{--}30P_x$ (corresponding to $10\text{--}15P_0$, or approximately $100\text{--}150\text{ kg cm}^{-2}$) (Fig. 3B); the marked load-bearing ability was still observed even when the catch force was reduced to $0.2P_0$.

If, on the other hand, the load applied to the ABRM fibres exceeded $10\text{--}15P_0$ (or $15\text{--}30P_x$), they were lengthened rapidly by 10% of L_0 within 1 s after the load application, so that the lever, to which the preparation was hooked, came in contact with stop 3, which was fixed in position (see Fig. 1). As the result, the load was supported by stop 3 but not by the

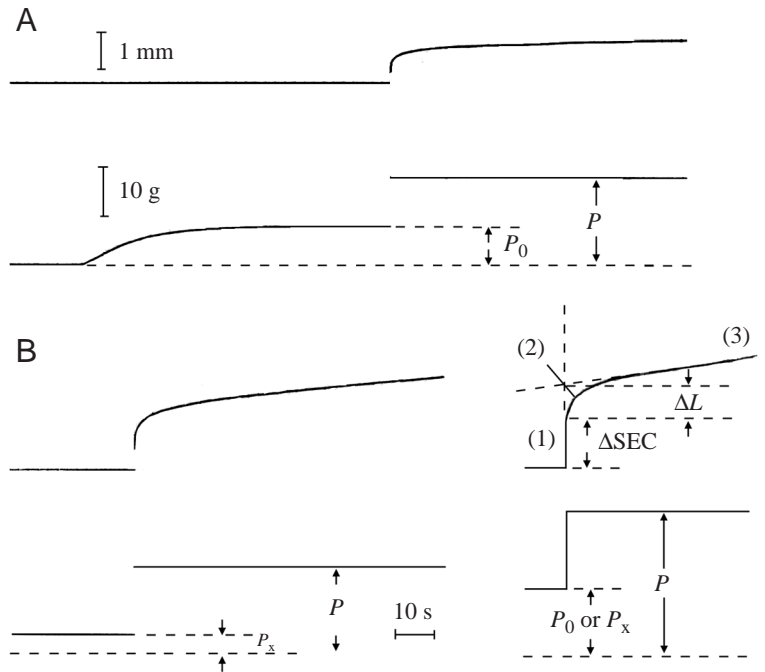


Fig. 2. Mechanical responses of the ABRM fibres to quick increases in load. The load on the preparation increased from P_0 to P ($\sim 2.3P_0$) in A, and from P_x ($\sim 0.5P_0$) to P ($\sim 4.5P_x$) during the catch state in B. In this and the subsequent figures, the upper and lower traces show length and force changes, respectively. Bottom broken lines represent zero force level. Records A and B were obtained from the same preparation. Inset illustrates the three phases (1–3) of the mechanical response as well as the method to determine the amplitude of the early isotonic lengthening ΔL . SEC, series elastic component.

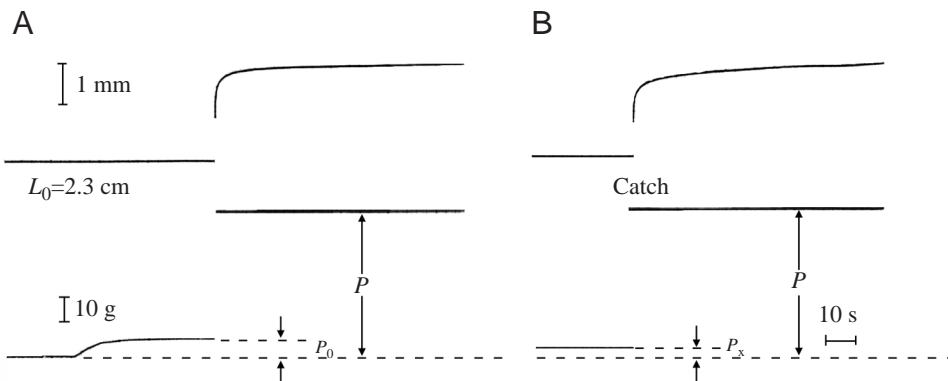


Fig. 3. Marked load-bearing ability of the ABRM fibres during the maximum active force generation (A) and during the catch state (B). The load was increased from P_0 to P ($\sim 8P_0$) in A, and from P_x ($\sim 0.5P_0$) to P ($\sim 16P_x$) in B. Records A and B were obtained from the same preparation.

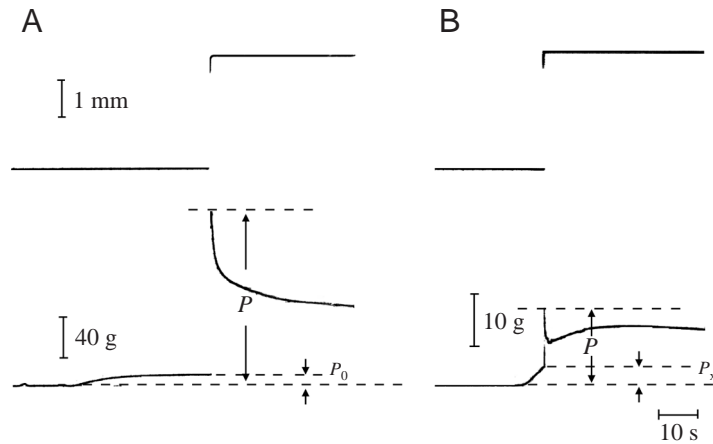


Fig. 4. 'Give' in the ABRM fibres following quick increases in load applied during the maximum active force generation (A) and during the early phase of ACh-induced force development (B). The amount of load P was $\sim 1.5P_0$ in A and $\sim 1.5P_0$ ($\sim 4P_x$) in B. Records A and B were obtained from different preparations.

preparation, and the subsequent force changes in the preparation showed the time course of stress relaxation, i.e. decay of the force in the preparation after completion of lengthening (Fig. 4A). The rapid ABRM fibre lengthening under a large load is thought to correspond to 'give' in the vertebrate skeletal muscle fibres. After showing 'give', the preparation could still develop full isometric force P_0 when again stimulated with ACh, indicating that the 'give' was associated with rapid slippage of linkages in the contractile system but not with any irreversible damage to the preparation.

Limited load-bearing ability of the ABRM fibres during the development of isometric force

When the load on the ABRM fibres was increased quickly during the early phase of ACh-induced force development (force level $P_x < 0.5P_0$), they were easily made to lengthen rapidly under small loads, as indicated by the appearance of stress relaxation of the force in the preparation immediately after completion of fibre lengthening (Fig. 4B). The 'give' of the preparation during the early phase of force development took place with loads above $1.5-2P_0$ or $3-4P_x$, which were comparable to those causing 'give' in skeletal muscle fibres (Katz, 1939; Sugi and Tsuchiya, 1981). This indicates that the linkages producing the early active force development can be made to slip rapidly with loads much smaller than those causing the rapid slippage of the linkages responsible for production of the maximum active force or the catch force. When the force developed above $0.5P_0$, the load-bearing ability increased abruptly with increasing force towards P_0 , though the time course was not studied in detail.

Dependence of the parameters of the mechanical response on the magnitude of quick increases in load

The parameters of the mechanical response of the ABRM fibres to quick increases in load are shown in Fig. 5 as

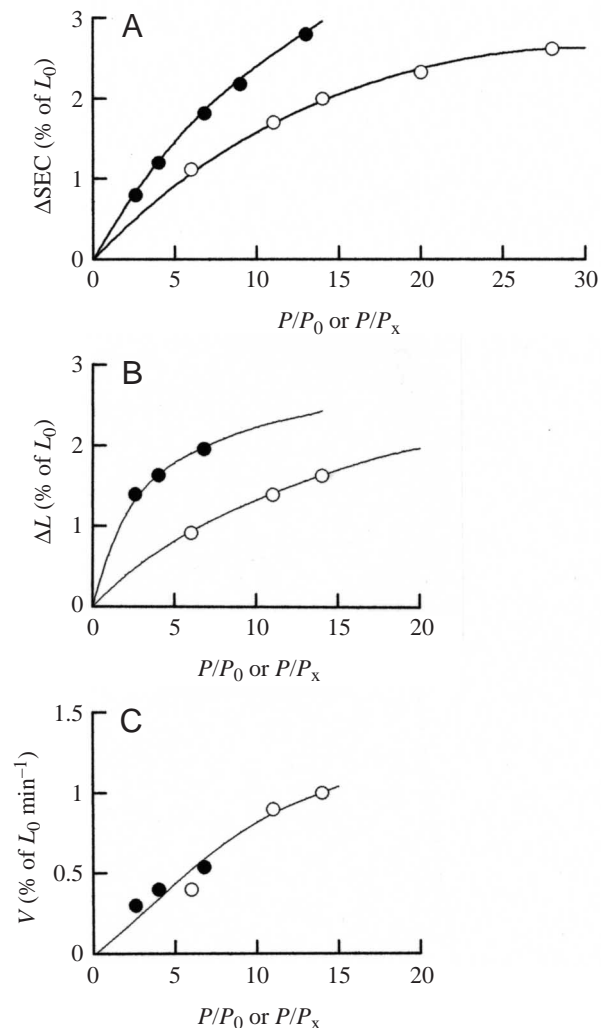


Fig. 5. Dependence of the extension of the series elastic component ΔSEC (A), the amplitude of the early isotonic lengthening ΔL (B), and the velocity of the late isotonic shortening V (C) on the amount of load P . Filled and open circles represent data points during the maximum active force generation and during the catch state, respectively. All data points are obtained from the same preparation.

functions of load P . All the data points were obtained on one and the same preparation, and similar results were obtained from 12 other preparations examined. In Fig. 5A, the amount of extension of the SEC (ΔSEC , expressed as percentage of L_0) is plotted against the magnitude of load (P expressed as a fraction or multiple of P_0 or P_x). Despite a large variation in the value of P_x , all data points obtained during the catch state fell on the same ΔSEC versus P curve. The value of ΔSEC for a given amount of P was smaller during the catch state (open circles) than during the maximum active force generation (filled circles), indicating that the SEC is stiffer during the catch state than during the maximum active force generation.

In Fig. 5B, the amplitude of the early isotonic lengthening ΔL is plotted against P . As the late steady fibre lengthening under large loads was terminated by stop 3 in 20–30 s after the load change, the velocity of steady isotonic lengthening (and

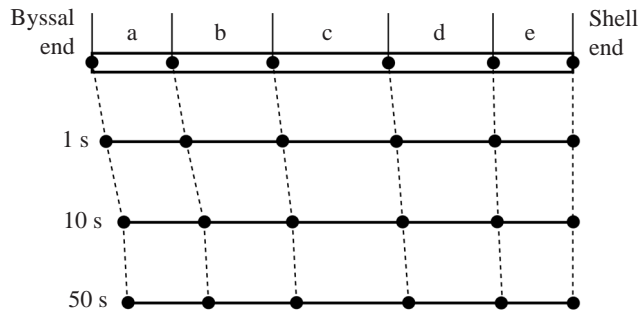


Fig. 6. Segmental length change of an ABRM fiber bundle ($L_0=2.4$ cm) at 1 s, 10 s and 50 s after a quick increase in load from P_0 to $6.5P_0$, applied during the maximum isometric force generation. The preparation was divided into five consecutive segments designated a, b, c, d and e.

therefore the value of ΔL could be determined accurately only under loads $<15P_0$. The data points in the catch state also fell around the same curve. As with the ΔSEC versus P relationship, the value of the ΔL for a given amount of P was smaller during the catch state than during the maximum active force generation, indicating that the ABRM fibres are less extensible during the catch state (open circles) than during the maximum active force generation (filled circles). Fig. 5C shows the relationship between the velocity V of the late steady isotonic lengthening and P . The value of V increased with increasing P , and the curve of V versus P appeared to be similar both during the maximum active force generation (filled circles) and during the catch state (open circles).

Segmental length changes of the ABRM fibres following quick increases in load

Measurement of the segmental length changes of the preparation following a quick increase in load indicated that the isotonic lengthening always took place uniformly along its entire length, as shown in Fig. 6. Even when the preparation exhibited 'give', i.e. rapid fibre lengthening under a large load (see Fig. 4), all fibre segments were uniformly lengthened (accuracy of measurement $<5\%$), indicating that 'give' was associated with uniform fibre lengthening but not with any localized lengthening of the weakest fibre segment. Similar results were obtained with three other preparations examined

Discussion

Evidence for the presence of the load-bearing system other than the actomyosin system in the ABRM fibres

The most remarkable finding in the present study is that the ABRM fibres exhibit extremely marked load-bearing ability both during the maximum isometric force generation and during the catch state (Fig. 3). If, however, quick changes in load were applied during the early phase of active force development, the ABRM fibres readily exhibited 'give' under small loads (Fig. 4B). Since the load causing 'give' of the ABRM fibres during the early phase of force development is

nearly equal to the load causing 'give' in vertebrate skeletal muscle fibres (Katz, 1939; Sugi and Tsuchiya, 1981), the early force development could be due to the actomyosin system, i.e. actin-myosin linkages between actin on the thin filament and myosin on the paramyosin-containing thick filament (Squire, 1981). On the other hand, the extremely marked load-bearing ability of the ABRM fibres observed both during the maximum active force generation and during the catch state (Fig. 3) is several times larger than that of vertebrate skeletal muscle fibres, and is unlikely to be due to the actomyosin system. Therefore, the present results can most readily be accounted for in terms of two independent systems acting in parallel with each other; one is the actomyosin system associated with actin-myosin linkages, while the other is the force-bearing system producing the marked load-bearing ability.

During the ACh-induced active contraction of the ABRM fibres, the maximum shortening velocity V_{\max} is largest during the isometric force development, and is reduced to about one-third (from $\sim 0.25L_0 \text{ s}^{-1}$ to $\sim 0.08L_0 \text{ s}^{-1}$) when the force reaches P_0 (Tameyasu and Sugi, 1976). This may be due to a slowing of cycling of actin-myosin linkages during the course of contraction, or alternatively, to a special force-bearing system, which is gradually built up during the course of active force development. When the active force is maximum, the force-bearing structure may be fully built up to produce a load-bearing ability far greater than that expected from actin-myosin linkages; the reduction of V_{\max} at P_0 may result either from an increased internal resistance against shortening due to the force-bearing structure and/or from a decrease in the number of actin-myosin linkages. When the catch state is established, the force may only be maintained by linkages of the load-bearing system.

Physiological role of the load-bearing system

The build-up of the load-bearing structure during the active force development, as revealed in the present work, can be understood well by considering how a typical catch muscle, for example the adductor muscle of a bivalve, works in its natural environment. When the animals are attacked by natural enemies, they rapidly close their shells by active shortening of the adductor muscle, and as soon as the shell is closed the adductor muscle resists against external forces acting to open the shell. To be able to do this, the force-bearing structure should be built up during the period of active muscle shortening produced by actin-myosin sliding. After the shell is closed, the adductor muscle may gradually go into the catch state, in which the marked load-bearing ability is well maintained only by the load-bearing structure, with an extremely small rate of energy consumption. This idea is supported by the reports that actomyosin ATPase activity is absent in the ABRM during the catch state (Güth et al., 1984; Galler et al., 1999).

Relation with previous studies

The isotonic lengthening of ABRM fibres was studied by Sugi and Tsuchiya (1979), but they only focused attention on

early isotonic fibre lengthening with decreasing velocity, and overlooked the late isotonic lengthening. During the early isotonic shortening, i.e. during phase 2 (Fig. 2), the velocity of lengthening decreases markedly, and in the subsequent late isotonic lengthening the ABRM fibres can bear very large loads while being lengthened extremely slowly (Figs 2 and 3). This marked decrease in the lengthening velocity in early isotonic lengthening suggests that the build-up of the load-bearing structure is accelerated when the fibres are lengthened under a large load.

According to the two-component model (Hill, 1938), a muscle consists of the SEC and the contractile component (CC) connected in series. Jewell and Wilkie (1960) showed that the SEC in a muscle originates partly from connections of experimental apparatus, and partly distributes along the muscle length. The extension of the SEC in the experimental apparatus can now be minimized by using single fibres or small fibre bundle preparations, and by reducing compliance of the experimental apparatus. In single skeletal muscle fibres, the extension of the SEC under P_0 is about 1% of the fibre length L_0 , corresponding to about 10 nm per half-sarcomere. The SEC in skeletal muscle fibres is therefore interpreted to largely originate from the elasticity of actin–myosin linkages (Huxley and Simmons, 1971). In the ABRM fibres, the extension of the SEC under P_0 is about 2% of L_0 (Tameyasu and Sugi, 1976; Sugi and Tsuchiya, 1979). Based on the very long lengths of thick and thin filaments in the ABRM (Gilloteaux and Baguet, 1977; Squire, 1981), the functional and structural unit in the ABRM, corresponding to the half-sarcomere in skeletal muscle, is very long, being of the order of 10 μm . The extension of the SEC at P_0 is therefore too large to be explained by extension of actin–myosin linkages. Since the SEC has been shown to distribute uniformly along the entire length of the ABRM fibres (Sugi and Tsuchiya, 1979), it may originate from some elastic structures uniformly distributed along the fibre length, and is uniformly extended by forces generated by the CC.

The force–extension curve of the SEC with forces $<P_0$ in the ABRM was studied by Lowy and Millman (1963) and Tameyasu and Sugi (1976). They reported that the curve obtained during the maximum active force generation was the same in shape as that obtained during the catch state, provided the catch tension was relatively high ($\geq 0.5P_0$). This was interpreted as evidence that both the active and catch forces are produced by the same contractile system, i.e. actin–myosin linkages. Recently, however, Sugi et al. (1999) have shown that the SEC in the ABRM fibres becomes definitely stiffer in the late phase of the catch state, in which the catch force decays below $0.5P_0$, which is consistent with the presence of a force-bearing structure other than the actomyosin system. In the present study, the force–extension curves of the SEC for forces $>P_0$ were obtained by applying quick increases in load, and the SEC has also been shown to be definitely stiffer during the catch state than during the maximum active force generation (Fig. 5A). This is consistent with the idea that the ABRM fibres contain linkages of both the actomyosin and the load-bearing

systems during the maximum active force generation, while they contain only linkages of the latter during the catch state.

The same argument would apply for the ΔL versus P relationship (Fig. 5B); the result that the increase of ΔL with increasing P is less marked in the catch state than during the maximum active force generation (Fig. 5B) may be taken to indicate that linkages associated with the load-bearing system can be made to slip less readily under large loads than actin–myosin linkages. During the late slow isotonic lengthening, on the other hand, the V versus P relation appeared to be the same during both the active force generation and the catch state (Fig. 5C). This might result from the fact that only linkages of the load-bearing system are responsible for the extremely slow isotonic lengthening of the ABRM fibres, while actin–myosin linkages are dissociated during the period of early isotonic lengthening.

Based on the linkage hypothesis, on the other hand, Butler et al. (1998, 2001) suggest that the catch state results from conversion of cycling actin–myosin linkages into non-cycling ones caused by dephosphorylation of twitchin, a high molecular mass protein known to occur in the ABRM (Siegman et al., 1997). However, their hypothesis explains neither the large load-bearing ability of non-cycling linkages nor the rapid development of large load-bearing ability that should be coupled with rapid dephosphorylation of twitchin.

Possible structural basis of the load-bearing system

The extensive aggregation of the thick filament in the ABRM during the catch state has been reported by many authors (Heumann and Zebe, 1968; Gilloteaux and Baguet 1977; Hauk and Achazi, 1987). Although the marked thick filament aggregation reported by them is claimed to be an artefact due to glutaraldehyde cross-linking of lysine residues on the thick filament, such a cross-linking may take place only when the distance between the thick filaments gets closer in the catch state. In fact, ABRM fibres quickly frozen in the catch state exhibit abundant thick filament interconnections (Takahashi et al., 2003). The decreased distance between the thick filaments caused by the formation of the thick filament interconnections might result in the thick filament aggregation, if the ABRM is fixed in the catch state with glutaraldehyde.

Although the arrangement of twitchin on the thick filament of the ABRM is unknown, it seems possible that it is twitchin that interconnects the thick filament to build up the force-bearing system. To clarify the arrangement of twitchin in the ABRM thick filaments, we are currently performing high-resolution scanning electron microscopy of the thick filaments in quick-frozen ABRM fibres, in the hope of proving that the thick filament interconnections are actually responsible for the marked load-bearing ability.

References

- Atsumi, S. and Sugi, H. (1976). Localization of calcium-accumulating structures in the anterior byssal retractor muscle of *Mytilus edulis* and their

- role in the regulation of active and catch contractions. *J. Physiol.* **257**, 549-560.
- Baguet, F.** (1973). The catch state in glycerol extracted fibers from a lamellibranch smooth muscle. *Pflügers Arch. Eur. J. Physiol.* **340**, 19-34.
- Baguet, F. and Gillis, J. M.** (1968). Energy cost of tonic contraction in a lamellibranch catch muscle. *J. Physiol.* **198**, 127-143.
- Bennett, P. M. and Elliott, A.** (1989). The 'catch' mechanism in molluscan muscle: an electron microscopy study of freeze-substituted anterior byssus retractor muscle of *Mitilus edulis*. *J. Muscle Res. Cell Motil.* **10**, 297-311.
- Butler, T. M., Mooers, S. U., Narayan, S. and Siegman, M. J.** (1998). Regulation of catch muscle by twitchin phosphorylation: effect on force, ATPase, and shortening. *Biophys. J.* **75**, 1904-1914.
- Butler, T. M., Narayan, S., Mooers, S. U., Hartshorne, D. and Siegman, M. J.** (2001). The myosin crossbridge cycle and its control by twitchin phosphorylation in catch muscle. *Biophys. J.* **80**, 415-426.
- Galler, S., Kogler, H., Ivemeyer, M. and Rüegg, J. C.** (1999). Force response of skinned molluscan catch muscle following photolibration of ATP. *Pflügers Arch. Eur. J. Physiol.* **438**, 525-530.
- Gilloteaux, J. and Baguet, F.** (1977). Contractile filaments organization in functional states of the anterior byssus retractor muscle (ABRM) of *Mytilus edulis* L. *Cytobiol.* **15**, 192-220.
- Güth, K., Gangelmann, M. and Rüegg, J. C.** (1984). Skinned smooth muscle: time course of force and ATPase activity during contraction cycle. *Experientia* **40**, 174-176.
- Hauk, R. and Achazi, R. K.** (1987). The ultrastructure of a molluscan catch muscle during a contraction-relaxation cycle. *Eur. J. Cell Biol.* **45**, 30-35.
- Heumann, H. G. and Zebe, E.** (1968). Bei die Functionweise glatter Maskelfasern, Elektronenmikroskopische Untersuchungen am Byssusretraktor (ABRM) von *Mitilus edulis*. *Z. Zellforsch.* **85**, 534-551.
- Hill, A. V.** (1938). The heat of shortening and dynamic constants of muscle. *Proc. R. Soc. B* **126**, 136-195.
- Huxley, A. F. and Simmons, R. M.** (1971). Proposed mechanism of force generation in striated muscle. *Nature* **233**, 533-538.
- Ishii, N., Simpson, A. W. M. and Ashley, C. C.** (1989). Free calcium at rest and during 'catch' in single smooth muscle cells. *Science* **243**, 1367-1368.
- Jewell, B. R.** (1959). The nature of the phasic and the tonic responses of shortening of the anterior byssal retractor muscle of *Mytilus*. *J. Physiol.* **149**, 154-177.
- Jewell, B. R. and Wilkie, D. R.** (1960). An analysis of the mechanical components in frog's striated muscle. *J. Physiol.* **143**, 515-540.
- Johnson, W. H., Kahn, J. S. and Szent-györgyi, A. G.** (1959). Preparation and contraction of 'catch' muscles. *Science* **130**, 160-161.
- Katz, B.** (1939). The relation between force and speed in muscular contraction. *J. Physiol.* **96**, 45-64.
- Kobayashi, T., Kosuge, S., Narushima, K. and Sugi, H.** (1998). Evidence for two distinct cross-bridge populations in tetanized frog muscle fibers stretched with moderate velocities. *Biochem. Biophys. Res. Commun.* **249**, 161-165.
- Lowy, J. and Millman, B. M.** (1963). The contractile mechanism of the anterior byssus retractor muscle (ABRM) of *Mitilus edulis*. *Phil. Trans. R. Soc. Lond. B* **246**, 105-148.
- Miller, A.** (1968). A short periodicity in the thick filaments of the anterior byssus retractor muscle of *Mitilus edulis*. *J. Mol. Biol.* **32**, 687-688.
- Nauss, K. M. and Davies, R. E.** (1966). Changes in inorganic phosphate and arginine during the development, maintenance and loss of tension in the anterior byssus retractor muscle of *Mitilus edulis*. *Biochem. Z.* **345**, 173-187.
- Siegman, M. J., Mooers, S. U., Li, C., Narayan, S., Trinkle-Mulcahy, L., Watabe, S., Hartshorne, D. J. and Butler, T. M.** (1997). Phosphorylation of a high molecular weight (~600 kDa) protein regulates catch in invertebrate smooth muscle. *J. Muscle Res. Cell Motil.* **18**, 655-670.
- Squire, J. M.** (1981). *The Structural Basis of Muscular Contraction*. New York: Plenum Press.
- Sugi, H., Iwamoto, H., Shimo, M. and Sirakawa, I.** (1999). Evidence for load-bearing structures specialized for the catch state in *Mytilus* smooth muscle. *Comp. Biochem. Physiol.* **122A**, 347-353.
- Sugi, H. and Tsuchiya, T.** (1979). The change in the load-sustaining ability and in the series elasticity in *Mytilus* smooth muscle during isotonic shortening. *J. Physiol.* **288**, 635-648.
- Sugi, H. and Tsuchiya, T.** (1981). Enhancement of mechanical performance in frog muscle fibres after quick increases in load. *J. Physiol.* **319**, 239-252.
- Takahashi, I., Shimada, M., Akimoto, T., Kishi, T. and Sugi, H.** (2003). Electron microscopic evidence for the thick filament interconnectons associated with the catch state in the anterior byssal retractor muscle of *Mytilus edulis*. *Comp. Biochem. Physiol.* **64**, 479-510.
- Tameyasu, T. and Sugi, H.** (1976). The series elastic component and the force-velocity relation in the anterior byssal retractor muscle of *Mytilus edulis*. *J. Exp. Biol.* **134A**, 115-120.
- Twarog, B. M.** (1954). Response of a molluscan smooth muscle to acetylcholine and 5-hydroxytryptamine. *J. Cell. Comp. Physiol.* **44**, 141-163.